Journal of Alloys and Compounds 509 (2011) 3740–3745

Contents lists available at ScienceDirect

Journal of Alloys and Compounds

journal homepage: www.elsevier.com/locate/jallcom

Quantitative elemental analysis of nickel alloys using calibration-based laser-induced breakdown spectroscopy

G.P. Gupta[a,*], B.M. Suri[a], A. Verma[b], M. Sundararaman[b], V.K. Unnikrishnan[c], K. Alti[c], V.B. Kartha[c], C. Santhosh[c]

[a] Laser & Plasma Technology Division, Bhabha Atomic Research Centre, Trombay, Mumbai 400085, Maharashtra, India
[b] Structural Metallurgy Section, Materials Group, Bhabha Atomic Research Centre, Mumbai, India
[c] Centre for Atomic and Molecular Physics, Manipal University, Manipal 576104, India

ARTICLE INFO

Article history:
Received 25 August 2010
Accepted 28 December 2010
Available online 5 January 2011

Keywords:
LIBS
Nickel alloys
Internal standardization
Calibration curve

ABSTRACT

This work reports on the quantitative elemental analysis of nickel alloys using laser-induced breakdown spectroscopy (LIBS) in air at atmospheric pressure. The LIBS plasma is generated using a Q-switched ultraviolet Nd:YAG laser, which evolves with time. The LIBS spectra of three samples with known composition are recorded at five detector gate delays. Employing the internal standardization method, the calibration curves for Cr present in the samples are produced. The Cr concentration in the samples is determined using the generated linear calibration curves having varying slopes and regression coefficients at different delays. The effect of slopes and regression coefficients of the linear calibration curves on the analytical predictive capability of the LIBS system is studied through the correlation of the LIBS determined concentration of Cr with its known value. The analytical predictive capability of the LIBS system is noted to be the best when the calibration-based analysis is performed at an appropriate delay (2000 ns in the present experiment) where the linear calibration curve has both the regression coefficient and the slope close to the ideal value.

1. Introduction

Laser-induced breakdown spectroscopy (LIBS) [1,2] has been well recognized as a simple, fast and direct analytical technique of elemental analysis of multi-element materials by a number of research groups all over the world. It is based on the focusing of a high-power pulsed laser beam with a power density >100 MW/cm^2 onto a sample surface followed by optical emission spectroscopy of the plasma produced over the surface. The LIBS technique has well-known attractive features over other widely used analytical techniques of atomic emission spectroscopy. In particular, vaporization and excitation of samples are possible in a single step and no restriction has to be placed on the sample size or specific requirement of sample preparation. Moreover, simultaneous multi-element analysis can be performed irrespective of atomic number of elements and this technique can be employed for online analysis remotely in hostile environments. During the last two decades, LIBS has attracted a lot of attention, leading to an ever-increasing list of applications, both in laboratory and in industry. One of the major applications of this technique is in the composition analysis of metallic materials [3].

For quantitative elemental analysis of unknown samples, the calibration curve, which is a plot of intensity of an analyte emission line versus its concentration, is commonly made with standards of known elemental concentrations in a matrix close to that of the unknown samples. Although the calibration curve method is the convenient approach for quantitative analysis, it is most suited for matrix-matched samples. For achieving accurate quantitative results from the linear calibration curves, the experimental conditions affecting the analytical performance need to be carefully studied [4–6]. The slope of the calibration curve that represents the sensitivity and the regression coefficient of the calibration curve that represents the precision are the two important parameters affecting the analytical predictive capability of the LIBS system to unknown samples. Several LIBS research papers on metallic solid samples in air at atmospheric pressure have been published in the literature where the calibration curves are obtained with varying slopes and regression coefficients [6–15]. But, to the best of our knowledge, their effect on the correlation of the LIBS determined concentration with that determined by any other analytical method is not reported in the literature.

In the present work, we have produced calibration curves for Cr, at five values of the detector gate delay relative to the laser pulse, from the LIBS spectra of three samples of nickel alloys with known composition in air at atmospheric pressure using a nanosecond, ultraviolet Nd:YAG laser, employing the internal standardization

* Corresponding author. Tel.: +91 22 25595058; fax: +91 22 25505151.
E-mail address: gpgupta@barc.gov.in (G.P. Gupta).

0925-8388/$ – see front matter © 2011 Elsevier B.V. All rights reserved.
doi:10.1016/j.jallcom.2010.12.189

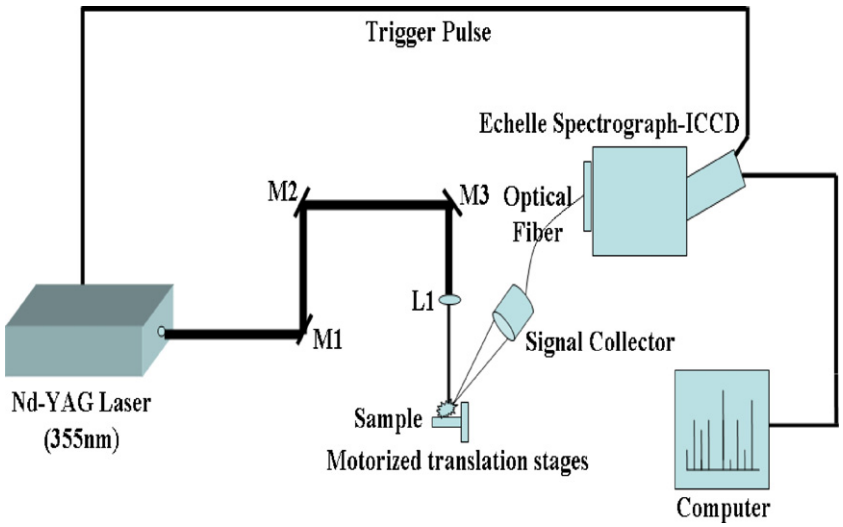

Fig. 1. Schematic diagram of the experimental set-up for LIBS studies.

(IS) method [10–12]. We have used the ultraviolet laser because it generates plasmas of samples in atmospheric air with improved emission characteristics [16]. We have investigated the effect of slopes and regression coefficients of the linear calibration curves that vary with the detector gate delay, on the quantitative elemental analysis considering three certified samples as unknown samples. We have discussed the influence of these two parameters of the linear calibration curve on the analytical predictive capability of the LIBS system.

2. Experimental

A schematic diagram of the experimental set-up for LIBS studies is shown in Fig. 1. A Q-switched Nd:YAG laser (Spectra Physics PRO 230-10) working at the third harmonic wavelength of 355 nm with a 6 ns pulse duration and a 10 Hz repetition rate was focused at right angles on the sample surface, placed in air at atmospheric pressure using a bi-convex lens of focal length 20 cm. For an estimated value of the diameter of the focussed beam of ~120 μm, the laser pulse irradiance on the sample surface was about 1.5×10^{10} W/cm^2. The sample was placed on a X–Y translation stage having speed 6 mm/s so that each laser pulse was incident on a fresh surface, thus maintaining the sample in the same conditions for different measurements. The spatially integrated plasma light emission was collected and imaged on to the spectrograph slit using an optical-fibre-based collection system. This collection system was positioned at a distance of about 20 cm from the plasma, making an angle 45° to the laser beam. An Echelle spectrograph-ICCD system (Andor Mechelle ME5000-DH734-18U-03PS150) was used to record the emission spectrum. The spectrograph, with an Echelle grating, covers 200–975 nm spectral range in a single shot with a good wavelength resolution (0.05 nm). The dispersed light from the spectrograph was collected by a thermoelectrically cooled ICCD camera which is sensitive in the whole UV–VIS–NIR spectral region converting the spectral signal into digital signal. A Hg–Ar lamp, which provides sharp lines from 200 to 1000 nm, was used for wavelength calibration of this system. Intensity calibration of the Echelle spectrograph-ICCD system was done using NIST certified deuterium–quartz–tungsten–halogen lamp (Ocean Optics, USA).

The detector was gated in synchronization with the laser pulse to get maximum signal-to-background (S/B) ratio. The detector gate width of 6 μs, which was found to be most advantageous in terms of the S/B ratio, was kept constant. The detector gate delay was varied in the time span 300–2000 ns for recording the plasma emission signals, discriminating the continuum radiation which is intense at initial delay times less than 300 ns and decreases at later times. We used a large detector gate width as used by Davies et al. [11] rather than a narrow gate width commonly used by various research groups, in order to enhance the S/B ratio. All LIBS spectra are derived from an integration of 120 laser pulses for obtaining enough reproducibility of the spectra.

For the present LIBS experiments, we have employed three samples of Ni_2 (Cr, Mo) alloys whose elemental compositions are listed in Table 1. These nickel alloys are prepared by melting Ni (99.99% purity), Cr (99.99% purity) and Mo (99.99% purity) in appropriate ratio in a non-consumable arc furnace with tungsten electrode and a water-cooled copper hearth under purified argon atmosphere. These compositions were chosen so that the alloys are in the single phase region in the ternary phase diagram. The alloys were homogenized at 1200 °C for 24 h in flowing argon atmosphere followed by furnace cooling and then hot rolled to about 0.5 mm thickness. The specimens from these alloys of 5 mm × 5 mm dimension were solution treated at 1150 °C for 2 h. X-ray diffraction as well as transmission microscopy studies confirmed that all the specimens are in single phase. Electron probe microanalysis also confirmed that the alloys have the same compositions as concentration of elements used for alloy preparation.

3. Results and discussion

3.1. LIBS spectra

Typical LIBS spectra of one of the certified Ni-alloy samples (sample 1) recorded at 2000 ns delay relative to the laser pulse are displayed in Fig. 2(a) and (b). The spectral lines of Cr I and Ni I of interest are shown in the inset of the figure. Three sets of such spectra are recorded for all the samples at each of the five delays of interest. A mean value calculated from the three spectra is used for the emission intensity of atomic lines, needed for obtaining the calibration curves.

3.2. Selection of spectral lines

The selection of the spectral lines of the analyte element as well as the internal standard (reference) element is required to be carefully made for the reproducibility of the analytical results using the IS method [10–12]. As stated in [10–12], the spectral lines of both the analyte element and the reference element selected for the calibration curves should fulfill the four conditions: (i) they should be reasonably strong and isolated to avoid interference with other spectral lines, (ii) they should be non-resonant lines with lower levels much above the ground level particularly at higher concentrations of the elements of interest to avoid saturation of emission intensities due to self-absorption of the emission lines, (iii) they should have the upper levels with energies close to each other such that their energy level difference is near zero (<2000 cm^{-1}) to minimize the plasma temperature effect on the reproducibility of the line intensity ratio and (iv) they should be simultaneously detected in a single laser shot to avoid complexities in the line

Table 1
Elemental concentrations (wt%) in three certified samples of Ni_2 (Cr, Mo) alloys.

Sample	Cr	Mo	Ni
1	16.67	16.67	66.66
2	21.01	12.33	66.66
3	25.01	8.33	66.66

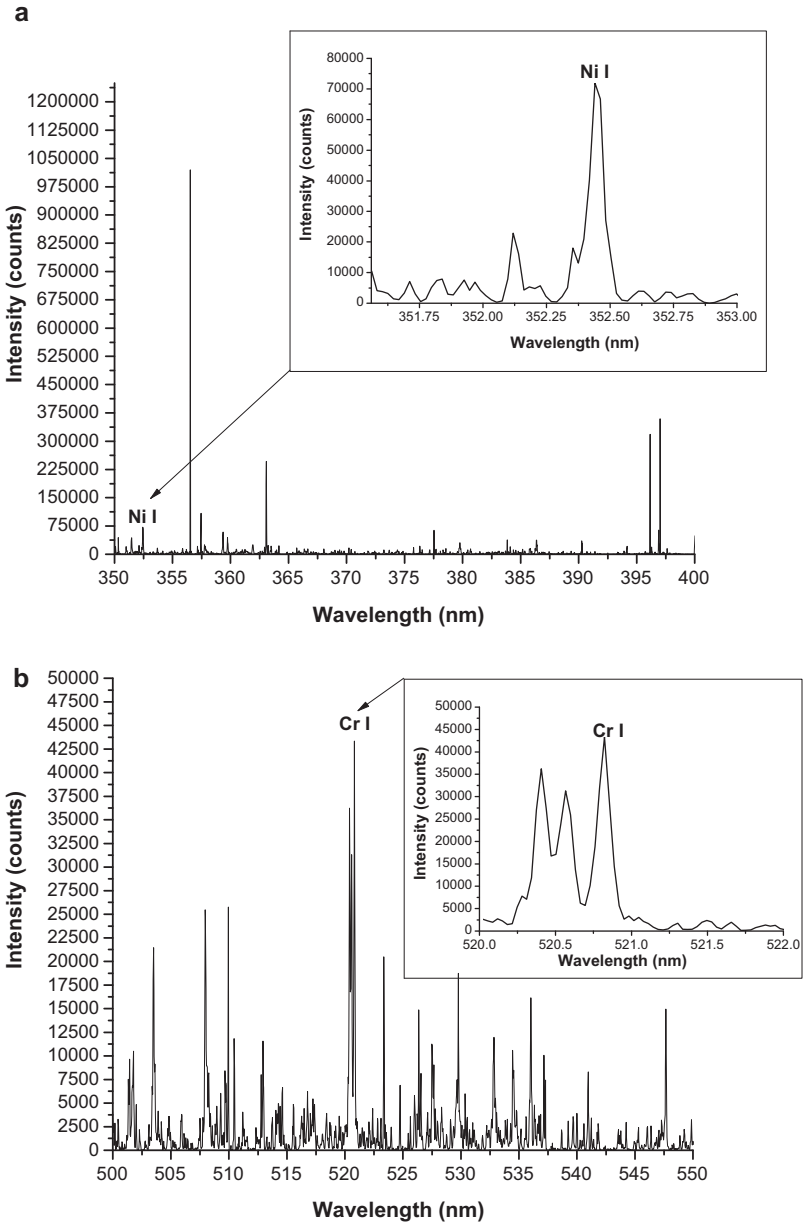

Fig. 2. Typical LIBS spectra of a Ni alloy (certified sample 1) at 2000 ns delay with inset showing Ni I line at 352.45 nm of interest (a) and with inset showing Cr I line at 520.84 nm of interest (b).

intensity calibration. The foremost requirement of similar upper level energies of the analyte and reference lines is not fulfilled in many LIBS works based on calibration curves [6,10–12], affecting slope and regression coefficient of the calibration curves. For the calibration curves of Cr using the IS method, we have chosen the analyte Cr and the reference Ni lines as shown in Table 2. The related spectroscopic parameters of the spectral lines, taken from the NIST atomic database [17], are also shown in the table. The energy level difference of the upper levels of the chosen line pairs is about 1780 cm^{-1}, thus satisfying the first requirement. These lines are non-resonant as well as interference-free, thus satisfying the second and third requirements. The fourth condition is automatically satisfied because the spectral range detected in a single laser shot using the present LIBS system is very large, covering the chosen line pairs.

Table 2
Atomic emission lines used for quantitative analysis, along with the related spectroscopic parameters.

Element	Species	Wavelength (nm)	Transition	
			Lower level energy (cm^{-1})	Upper level energy (cm^{-1})
Cr	Cr I	520.84	7593.2	26,787.5
Ni	Ni I	352.45	204.8	28,569.2

3.3. Quantitative analysis using the IS method

The quantitative analysis of the spectral emission from LIBS plasma involves relating the emission intensity of an atomic line of any element in the plasma to the concentration of that element in the sample. It relies on the assumption that the plasma is optically thin and in local thermodynamic equilibrium (LTE). Under this assumption, the intensity ratio of an atomic spectral line emitted by an analyte element (denoted by subscript a) to that emitted by the internal standard (reference) element (denoted by subscript r),

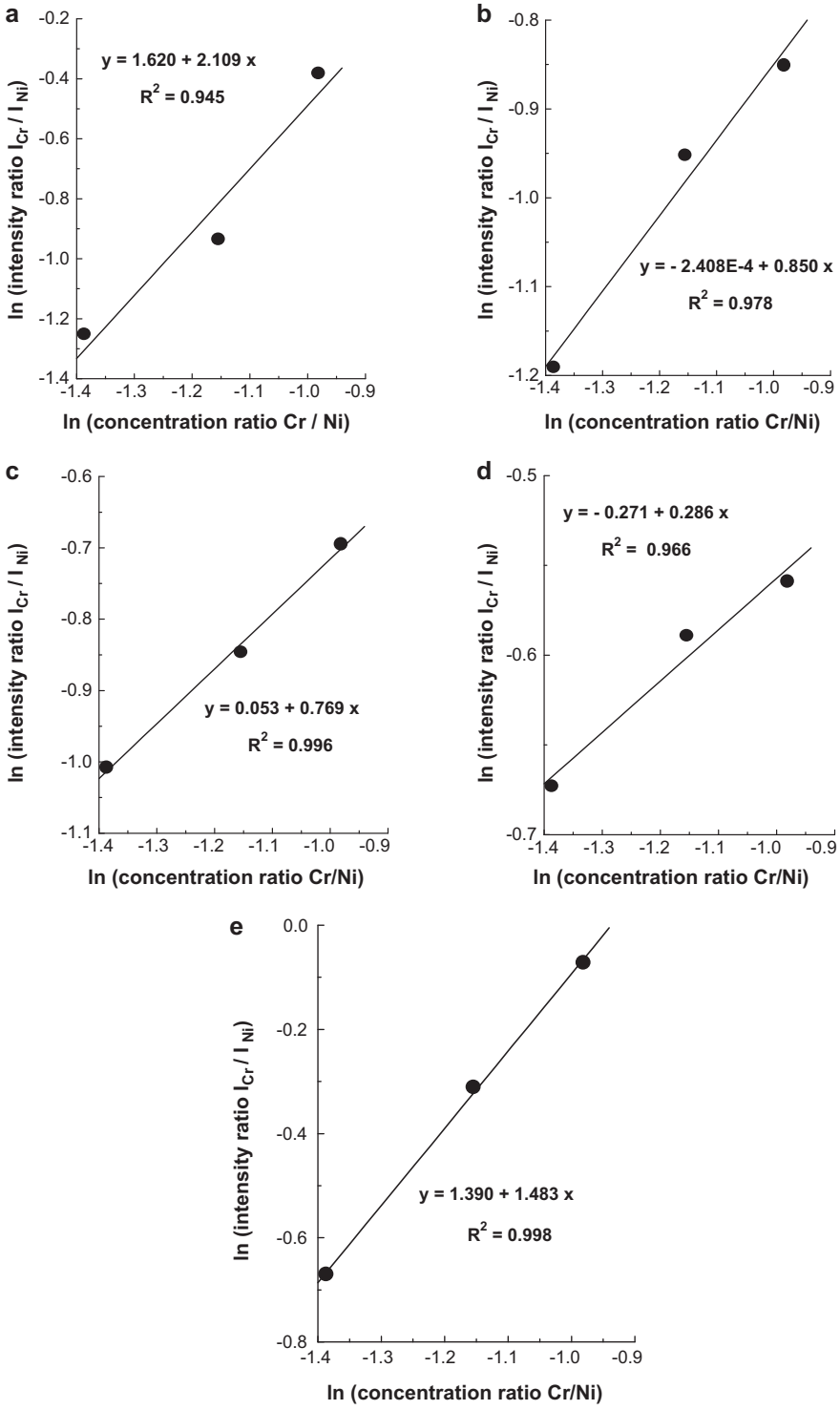

Fig. 3. Calibration curves for Cr at delay times 300 ns (a), 500 ns (b), 700 ns (c), 1000 ns (d) and 2000 ns (e). Linear regression equations and their coefficients are also given.

considered in the IS method, is given as [10–12,18]

$$\frac{I_a}{I_r} = \frac{N_a}{N_r}\frac{g_a}{g_r}\frac{A_a}{A_r}\frac{Z_r}{Z_a}\frac{\lambda_r}{\lambda_a}\exp\left[-\frac{(E_a - E_r)}{kT}\right] \quad (1)$$

Here I stands for the intensity of the spectral lines, N is the total atom number density, Z is the partition function, E and g are the energies and the degeneracies of the upper levels respectively, A and λ are the Einstein coefficient and the wavelength respectively for the observed line transitions, k is the Boltzmann constant and T is the plasma temperature.Taking the natural logarithms in Eq. (1), one obtains:

$$\ln\frac{I_a}{I_r} = \ln\frac{N_a}{N_r} + \ln\frac{g_a A_a Z_r \lambda_r}{g_r A_r Z_a \lambda_a} - \frac{E_a - E_r}{kT} \quad (2)$$

Thus, if the logarithm of the intensity ratio versus the logarithm of the concentration ratio is plotted, the calibration curve as a straight line with a slope of unity is obtained. Using the regression equation of the linear calibration curve one may obtain the analyte concentration from the measured analyte spectral intensity in unknown samples. Since the LIBS data are normally not per-

Table 3
Slope (m) and linear regression coefficient (R^2) of the calibration curves of Cr at five values of the detector gate delay using the three certified samples of Ni alloys.

Delay time (ns)	m	R^2
300	2.109	0.945
500	0.850	0.978
700	0.769	0.996
1000	0.286	0.966
2000	1.483	0.998

fectly reproducible, they do not fit perfectly on a straight line with regression coefficient equal to one. The slope values of the linear calibration curves are commonly observed to differ from the ideal slope of unity, owing to the inhomogeneity and matrix effect of the samples [10,18]. Both the regression coefficient and the slope of the linear calibration curve affect the analytical predictive capability of the LIBS system. When the energy difference of the upper energy levels is much smaller as compared to kT, the effect of the last term in Eq. (2) that contributes only to the intercept of this straight line, affecting the reproducibility of the spectral line intensity ratio, is negligible. Under this condition the intercept is determined by the second term on the right hand side of Eq. (2). Here all the components except Z remain constant for the selected lines, whereas Z is dependent on the plasma temperature.

3.4. Calibration curves for Cr

Using the analyte Cr and reference Ni lines given in Table 2 and Eq. (2), we have produced the calibration curves for Cr at five delay times and depicted these in Fig. 3. The logarithm of the relative intensity ratio of the analyte (Cr) element and the reference (Ni) element lines are plotted against the logarithm of the given relative concentrations of the three Ni alloy samples for the calibration curves of Cr. The linear regression equation and the regression coefficient for each of the calibration curves are also given in the figure. As seen from the figures, the calibration curves in our experiment are well characterized by a straight line without any saturation effect. The slopes and the regression coefficients of these linear calibrations curves are tabulated in Table 3. As evident from this table, the slope values differ from the ideal slope of unity, whereas the regression coefficient values of the linear fit are near unity with the best value equal to 0.998 at 2000 ns delay. From the regression equations, it is seen that the intercept varies widely over the delay times of interest. The radiative lifetimes of electronic energy levels are in ns, and the observation time of 6 μs more or less ensures that, for any delay, we observe the emissions from all the atoms reaching the levels involved. This intercept is varying from a positive value to zero to slightly negative, and then to positive. This change is ascribed to the dependence of Z on the plasma temperature that varies significantly with the delay time.

3.5. Analytical results

For the demonstration of analytical predictive capability of the present LIBS system, we have used the linear regression equations

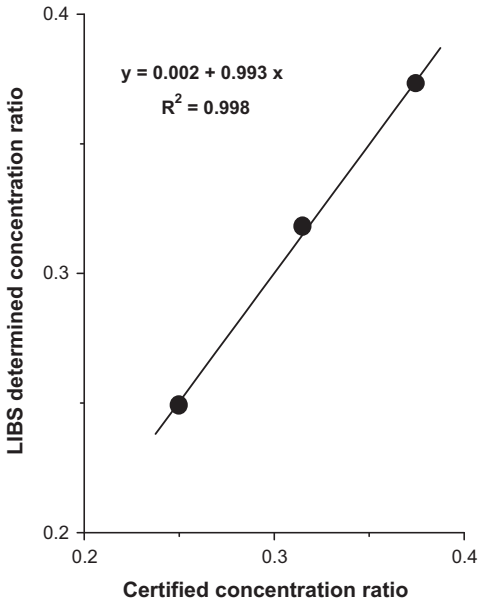

Fig. 4. Correlation of the LIBS determined concentration ratio Cr/Ni and certified concentration ratio Cr/Ni using the calibration curve at a delay time of 2000 ns.

of the produced calibration curves and determined the relative concentration of Cr in three nickel-alloy samples with known composition at 5 detector gate delays. We have also evaluated the accuracy of the elemental determinations using the LIBS method by their relative deviation from the certified values of the samples. Table 4 shows the correlation of the LIBS determined concentration ratio Cr/Ni with its certified value and the corresponding uncertainty of the three Ni-alloy samples using the produced calibration curves at 5 detector gate delays. It is observed that the high regression coefficient with its value very close to unity (0.998) along with the slope (1.483) of the linear calibration curve close to the ideal value of unity, obtained at 2000 ns gate delay in the present experiment, yields the best LIBS analytical results in all the three samples. Thus, the analytical predictive capability of the LIBS system is strongly dependent on both the slope and the regression coefficient of the calibration curve, the best capability occurring at a particular gate delay where both the slope and the regression coefficient of the linear calibration curve are close to the ideal value of unity. In Fig. 4, we have depicted the correlation of the LIBS determined concentration ratio Cr/Ni and certified concentration ratio Cr/Ni for the three Ni-alloy samples using the calibration curve at a delay time of 2000 ns where the correlation coefficient and the slope of the linear calibration curve are very close to the ideal value. As seen from the figure, the LIBS analytical results are fitted satisfactorily by a linear equation with the regression coefficient of 0.998 and the slope of 0.993. These results confirm high analytical predictive capability of the LIBS system provided the linear calibration curve is produced at an appropriate detector gate delay, having both the

Table 4
Correlation of the LIBS determined concentration ratio Cr/Ni with its certified value and the corresponding uncertainty of the three samples of Ni alloys using calibration curves at five values of the detector gate delay.

Sample	Certified concentration ratio Cr/Ni	LIBS determined concentration ratio Cr/Ni (correlation uncertainty, %)				
		Delay time (ns)				
		300	500	700	1000	2000
1	0.250	0.256 (2.4)	0.246 (1.6)	0.252 (0.8)	0.245 (2.0)	0.249 (0.4)
2	0.315	0.298 (5.4)	0.326 (3.5)	0.311 (1.3)	0.329 (4.4)	0.318 (1.0)
3	0.375	0.387 (3.2)	0.368 (1.9)	0.378 (0.8)	0.365 (2.7)	0.373 (0.5)

regression coefficient and the slope close to the ideal value of unity.

4. Conclusions

We have recorded the LIBS spectra of three Ni-alloy samples of known composition in air at atmospheric pressure using a Q-switched Nd:YAG ultraviolet laser at five detector gate delays with a view to investigate the effect of the slopes and the regression coefficients of linear calibration curves on the analytical predictive capability of the LIBS system. We have chosen the appropriate spectral lines of both the analyte and the reference elements, complying with the requirement of the IS method for the calibration curves. We have produced the calibration curves for Cr from the LIBS spectra, recorded at five detector gate delays, of three samples of nickel alloys and obtained the linear regression equations with their slopes and regression coefficients. Using these equations, we have determined the Cr concentration in three certified Ni-alloy samples from the measurement of its LIBS spectral intensity. We have studied the effect of slopes and regression coefficients of the linear calibration curves on the analytical predictive capability of the LIBS system through the correlation of the LIBS determined concentration of Cr with its certified value at five detector gate delays. The analytical predictive capability of the LIBS system is found to be the best when the linear calibration curve with regression coefficient and slope close to the ideal value corresponding to an appropriate detector gate delay, which occurred in the present experiment at 2000 ns gate delay, is utilized for the quantitative elemental analysis.

Acknowledgments

This work was carried out under the project titled “Trace Element Analysis for Environmental and Biomedical Applications – Development of Laser Induced Breakdown Spectroscopy (LIBS) Technique.” Project No. 2007/34/14-BRNS/87, Board of Research in Nuclear Sciences (BRNS), Department of Atomic Energy (DAE), Govt. of India.

References

[1] D.A. Cremers, L.J. Radziemski, Handbook of Laser-Induced Breakdown Spectroscopy, John Wiley & Sons Ltd., England, 2006.
[2] A.W. Miziolek, V. Pallesschi, I. Schechter (Eds.), Laser-Induced Breakdown Spectroscopy (LIBS), Cambridge University Press, New York, 2006.
[3] W.B. Lee, J.Y. Wu, Y.I. Lee, J. Sneddon, Appl. Spectrosc. 39 (2004) 27.
[4] X. Mao, W.-T. Chan, M. Caetano, M.A. Shannon, R.E. Russo, Appl. Surf. Sci. 96–98 (1996) 126.
[5] J.A. Aguilera, C. Aragon, F. Penalba, Appl. Surf. Sci. 127–129 (1998) 309.
[6] C. Aragon, J.A. Aguilera, F. Penalba, Appl. Spectrosc. 53 (1999) 1259.
[7] N. Andre, C. Geertsen, J.-L. Lacour, P. Mauchien, S. Sjostrom, Spectrochim. Acta, Part B 49 (1994) 1363.
[8] M. Sabsabi, P. Cielo, Appl. Spectrosc. 49 (1995) 499.
[9] A. Gonzalez, M. Ortiz, J. Campos, Appl. Spectrosc. 49 (1995) 1632.
[10] B. Bescos, J. Castano, A.G. Urena, Laser Chem. 16 (1995) 75.
[11] C.M. Davies, H.H. Telle, D.J. Montgomery, R.E. Corbett, Spectrochim. Acta, Part B 50 (1995) 1059.
[12] I. Bassiotis, A. Diamantopoulou, A. Giannoudakos, F.R. Kalantzopoulou, M. Kompitsas, Spectrochim. Acta, Part B 56 (2001) 671.
[13] L. Fornarini, F. Colao, R. Fantoni, V. Lazic, V. Spizzicchino, Spectrochim. Acta, Part B 60 (2005) 1186.
[14] A. De Giacombo, M. Dell’Aglio, O. De Pascale, R. Gaudiuso, R. Teghil, A. Santagata, G.P. Parisi, Appl. Surf. Sci. 253 (2007) 7677.
[15] B.C. Windom, D.W. Hahn, J. Anal. Atom. Spectrom. 24 (2009) 1665.
[16] K. Kagawa, K. Kawai, M. Tani, T. Kobayashi, Appl. Spectrosc. 48 (1994) 198.
[17] NIST Atomic Spectra Database, http://physics.nist.gov.
[18] R.S. Adrain, J. Watson, J. Phys. D: Appl. Phys. 17 (1984) 1915.